

# Cyclic voltammetry of cryptands and cryptates containing the ferrocene unit

C. Dennis Hall \*, Sunny Y.F. Chu

*Department of Chemistry, King's College London, Strand, London WC2R 2LS, UK*

Received 4 January 1995

## Abstract

Cyclic voltammetry studies of cryptands containing the ferrocene unit are reported, together with the shifts ( $\Delta E_{1/2}$ ) in redox potential caused by complex formation with a variety of monovalent, divalent and trivalent cations. Correlation between  $\Delta E_{1/2}$  values and the ratios charge ( $c$ )/cationic radius ( $r$ ) for amide cryptands or  $c/r^2$  for amine cryptands are rationalised in terms of the type of complex formed.

*Keywords:* Iron cryptands; Cryptates; Ferrocene; Cyclic voltammetry

## 1. Introduction

During the past decade we [1–11] and others [12–15] have reported the synthesis and characterisation of a wide range of macrocycles and cryptands containing metallocene units. One of the main objectives of this work was to observe the effect of cation complexation on the electrochemical properties of the host molecules, and to some extent this has been achieved for both the amide cryptands [16] and their amine analogues [17]. A variety of spectroscopic techniques including UV–vis spectroscopy, IR spectroscopy and multinuclear NMR coupled with X-ray crystallography have shown that in the case of the amide cryptands, the carbonyl group plays a major role in coordinating guest cations [10,11,18,19], whereas with the amine cryptands the cations are situated within the cavity [17,20]. Thus, in the case of the amides, transmission of electrical effects to the metallocene centre was expected to be through the carbonyl bonds connected to the Cp rings of the metallocene units but with the analogous amines one might expect the electrical effect to be “through space” and therefore to depend on the charge density on the cation and its proximity to the metallocene centre. This

hypothesis has been tested for a series of monomeric (1–4) and dimeric (5–8) cryptands (in the amide and amine form) with a range of mono-, di-, and trivalent cations and the results are reported below.

## 2. Experimental details

$^1\text{H}$  and  $^{13}\text{C}$  NMR spectra were recorded on either Bruker AM360 or Bruker WX400 spectrometers using  $\text{CDCl}_3$  or  $\text{CD}_2\text{Cl}_2$  as solvents. Cyclic voltammograms were recorded using an EG & G Model 273 potentiostat with Model 270 Software controlled by a Viglen computer connected to a Hewlett-Packard Colour Plotter for graphical output. The cyclic voltammetry (CV) experiments were conducted in dry  $\text{CH}_3\text{CN}$  as solvent with 0.1 M  $\text{Bu}_4\text{NClO}_4$  as supporting electrolyte,  $\text{Ag}/\text{AgNO}_3$  (0.01 M in  $\text{CH}_3\text{CN}$ ) as the reference electrode [21] and Pt wire as both working and counter electrodes. The scan rate was normally  $100\text{ mV s}^{-1}$  with IR compensation applied during each scan.

All the ferrocene-containing cryptands (1,3,5,7) were prepared as described elsewhere [2–4] and all showed the reported spectroscopic characteristics. They were reduced by slight modifications of the method of Gokel et al. [17] involving use of  $\text{LiAlH}_4$  in a mixture of  $\text{CH}_2\text{Cl}_2$  (5 parts) and THF (1 part) and the resultant

\* Corresponding author.

Table 1  
<sup>1</sup>H and <sup>13</sup>C NMR data on cryptands (2, 4, 6 and 8)<sup>a</sup>

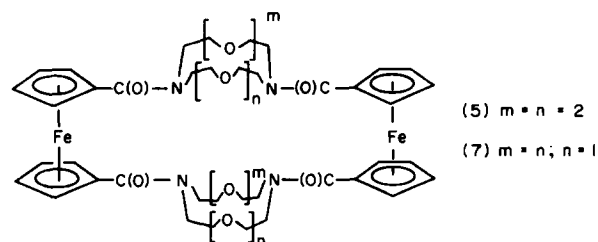
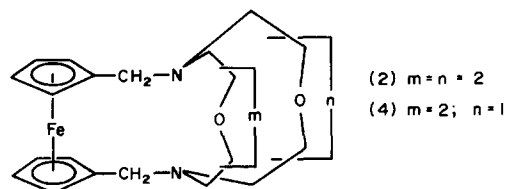
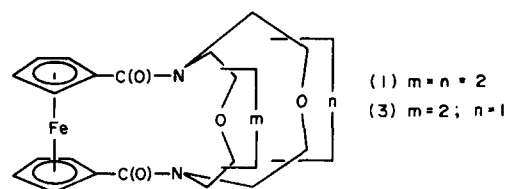
δ (ppm)	Integration (DEPT)	Assignment
<i>1,1'-(1,4,10,13-tetraoxa-7,16-diazacyclooctadecane-7,16-dimethylene)-ferrocene (2)</i>		
<sup>1</sup> H NMR (360 MHz)		
4.26 (t)	4	Cp
4.04 (t)	4	Cp
3.79 (m)	8	OCH <sub>2</sub>
3.66 (s)	4	Fc-CH <sub>2</sub> -N
3.64 (m)	8	OCH <sub>2</sub>
2.87 (m)	4	NCH <sub>2</sub>
2.65 (m)	4	NCH <sub>2</sub>
<sup>13</sup> C NMR (90.0 MHz)		
87.41	(0)	<i>ipso</i>
70.67	(-)	OCH <sub>2</sub>
69.90	(-)	OCH <sub>2</sub>
69.78	(+)	Cp
69.99	(+)	Cp
54.09	(-)	Fc-CH <sub>2</sub> -N
53.38	(-)	NCH <sub>2</sub>
<i>1,1',1',1'''-bis-(1,4,10,13-tetraoxa-7,16-diazacyclooctadecane-7,16-dimethylene)-bis-ferrocene (6)</i>		
<sup>1</sup> H NMR (360 MHz)		
4.08 (t)	2	Cp
4.07 (t)	2	Cp
3.64 (s)	4	OCH <sub>2</sub>
3.63 (s)	2	Fc-CH <sub>2</sub> -N
3.61 (t)	4	OCH <sub>2</sub>
2.72 (t)	4	NCH <sub>2</sub>
<sup>13</sup> C NMR (90.0 MHz)		
83.32	(0)	<i>ipso</i>
70.74	(+)	Cp
70.64	(-)	OCH <sub>2</sub>
69.37	(-)	OCH <sub>2</sub>
68.30	(+)	Cp
53.87	(-)	Fc-CH <sub>2</sub> -N
53.14	(-)	NCH <sub>2</sub>
<i>1,1'-(1,4,10-trioxa-7,13-diazacyclopentadecane-7,13-dimethylene)-ferrocene (4)</i>		
<sup>1</sup> H NMR (360 MHz)		
4.01–4.30 (broad)	8	Cp
3.78 (s) (broad)	4	Fc-CH <sub>2</sub> -N
3.38–3.82 (broad)	8	OCH <sub>2</sub>
2.35–3.11 (broad)	12	NCH <sub>2</sub>
<sup>13</sup> C NMR (90.0 MHz)		
78.22	(0)	<i>ipso</i>
70.50	(+)	Cp
70.08	(+)	Cp
69.60	(-)	OCH <sub>2</sub>
68.59	(+)	Cp
67.96	(+)	Cp
66.74	(-)	OCH <sub>2</sub>
66.49	(-)	OCH <sub>2</sub>
51.81	(-)	Fc-CH <sub>2</sub> -N
51.62	(-)	NCH <sub>2</sub>
50.66	(-)	NCH <sub>2</sub>

amines (2,4,6,8) were isolated by chromatography on alumina with CH<sub>2</sub>Cl<sub>2</sub>-MeOH (0.5%–1%) as eluant. Typical procedures are described below and the <sup>1</sup>H/<sup>13</sup>C NMR data for the amines are reported in Table 1.

Table 1 (continued)

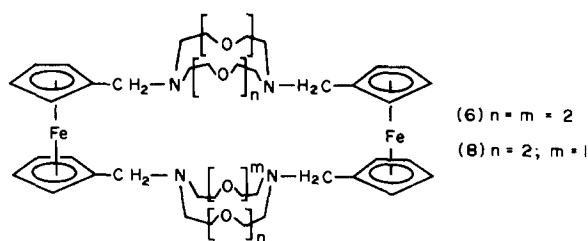
δ (ppm)	Integration (DEPT)	Assignment
<i>1,1',1',1'''-bis-(1,4,10-trioxa-7,13-diazacyclopentadecane-7,13-dimethylene)-bis-ferrocene (8)</i>		
<sup>1</sup> H NMR (360 MHz)		
4.09 (m)	2	Cp
4.04 (m)	2	Cp
3.58 (s)	2	Fc-CH <sub>2</sub> -N
3.52 (d)	6	OCH <sub>2</sub>
2.68 (t)	2	NCH <sub>2</sub>
2.64 (t)	2	NCH <sub>2</sub>
<sup>13</sup> C NMR (90.0 MHz)		
82.66	(0)	<i>ipso</i>
70.71	(+)	Cp
70.38	(+)	OCH <sub>2</sub>
70.19	(-)	Cp
69.93	(+)	OCH <sub>2</sub>
69.04	(+)	OCH <sub>2</sub>
68.60	(-)	Cp
68.41	(-)	Cp
56.77	(-)	Fc-CH <sub>2</sub> -N
55.30	(-)	NCH <sub>2</sub>
53.21	(-)	NCH <sub>2</sub>

<sup>a</sup> In CDCl<sub>3</sub> at 298 K.



## 2.1. Preparation of 1,1'-(1,4,10,13-tetraoxa-7,16-diazacyclooctadecane-7,16-dimethylene)-ferrocene (2)

LiAlH<sub>4</sub> (125 mg, 3.3 mmol) was added with vigorous stirring to a solution of 1,1'-(1,4,10,13-tetraoxa-



7,16-diazacyclooctadecane-7,16-diyl)ferrocene (500 mg, 1.0 mmol) in a mixture of anhydrous dichloromethane (20 ml) and tetrahydrofuran (THF) (4 ml) and the mixture was stirred under dinitrogen overnight at room temperature. The solution was then diluted with dichloromethane (25 ml) and treated with saturated aqueous sodium potassium tartrate (25 ml). The organic layer was separated, washed with water ( $3 \times 25$  ml) and dried over magnesium sulphate. The solvent was removed under vacuum, and the residue was chromatographed on alumina with  $\text{CH}_2\text{Cl}_2$ -0.5% MeOH as eluant. A pale yellow band was collected and the residue left after evaporation, was triturated with diethyl ether to afford a pale yellow powder (425 mg, 90% yield), m.p. 132–135°C, lit. [17] m.p. (2)  $\cdot \text{H}_2\text{O} = 101$ –104°C; RMM, thioglycerol matrix = 473 ( $M + 1$ ).

## 2.2. 1,1' : 1,1'''-bis-(1,4,10,13-tetraoxa-7,16-diazacyclooctadecane 7,16-dimethylene) bis-ferrocene (6)

The same procedure was used as for the monomer, except that the residue was chromatographed on alumina with  $\text{CH}_2\text{Cl}_2$ -1% MeOH as eluant. A pale yellow band was collected and upon removal of the solvents under vacuum yielded a pale yellow powder (70% yield m.p. 160–162°C, lit. [17] m.p. = 104–105°C); RMM, FAB, thioglycerol matrix = 945 ( $M + 1$ ).

## 2.3. 1,1'-(1,4,10-trioxa-7,13-diazacyclopentadecane-7,13-dimethylene)-ferrocene (4)

$\text{LiAlH}_4$  (50 mg, 1.3 mmol) was added with vigorous stirring to a solution of 1,1'-(1,4,10-trioxa-7,13-diazacyclopentadecane-7,13-diyl)ferrocene (200 mg, 0.40 mmol) in a mixture of anhydrous dichloromethane (10 ml) and THF (2 ml) and the mixture was stirred under dinitrogen for 30 min at room temperature. The solution was then diluted with dichloromethane (10 ml) and treated with saturated aqueous sodium potassium tartrate (20 ml). The organic layer was separated, washed with water ( $3 \times 20$  ml) and dried over magnesium sulphate. The solvent was removed under vacuum and the residue was chromatographed on alumina with  $\text{CH}_2\text{Cl}_2$ -0.5% MeOH as eluant. A pale yellow band was collected and on evaporation followed by recrystallisation

of the residue from diethyl ether afforded a pale yellow powder (100 mg, 60% yield, m.p. 128–130°C); RMM, FAB, thioglycerol matrix = 429 ( $M + 1$ ). Found: C, 61.34; H, 7.55; N, 6.33%; Calc. for  $\text{C}_{22}\text{H}_{32}\text{N}_2\text{O}_3$ : C, 61.68; H, 7.48; N, 6.54%.

## 2.4. 1,1' : 1,1'''-bis(1,4,10-trioxa-7,13-diazacyclopentadecane-7,13-dimethylene) bis-ferrocene (8)

The same procedure was used for the monomer, except that the residue was chromatographed on alumina with  $\text{CH}_2\text{Cl}_2$ -1% MeOH as eluant. A pale yellow band was collected which, upon removal of the solvents under vacuum yielded a pale yellow powder (40% yield, m.p. 156–158°C); RMM, FAB, thioglycerol matrix = 857 ( $M + 1$ ). Found: C, 61.27, H, 7.60; N, 6.40%; Calc. for  $\text{C}_{44}\text{H}_{64}\text{N}_4\text{O}_6$ , C, 61.68; H, 7.48; N, 6.54%.

## 2.5. Metal trifluoromethane sulphonates

All the trifluoromethane sulphonate salts were prepared by treatment of the appropriate metal carbonate or oxide with the stoichiometric amount of trifluoromethane sulphonic acid followed by evaporation of the residual water under high vacuum ( $< 0.01$  mm Hg) at 130°C.

## 3. Results and discussion

### 3.1. Cyclic voltammetry of (1) and (2) in the presence of metal trifluoromethane sulphonates

Cyclic voltammetry studies on the complexation of (1) with alkaline earth and lanthanide perchlorates were reported previously [16]. Here we have concentrated on a study of the complexation of (1) with alkali and alkaline earth trifluoromethane sulphonates together with the yttrium cation [as  $\text{Y}(\text{CF}_3\text{SO}_3)_3$ ] since it is similar in size to the sodium and calcium cations. The trifluoromethanesulphonates were chosen since they are readily soluble in acetonitrile and may be dried under vacuum at high temperature without risk of explosion.

A 2.0 mM solution of ligand (1) in  $\text{CH}_3\text{CN}/0.1$  M tetra-*n*-butylammonium perchlorate ( $\text{TBA}^+\text{ClO}_4^-$ ) gave one CV wave centred at 250 mV vs.  $\text{Ag}/\text{AgNO}_3$  (0.010 M in  $\text{CH}_3\text{CN}$ ), (Fig. 1(a)). The difference between the peak potentials ( $\Delta E_p$ ) was only 60 mV corresponding to reversible one-electron redox behaviour of the ferrocene unit. Although not all the cryptands (or cryptates) gave  $\Delta E_p = 60$  mV, the range was 60–100 mV and plots of peak current vs. the square root of the scan rate were all linear, thus denoting reversibility of each redox reaction. Addition of a substoichiometric amount of  $\text{Y}(\text{CF}_3\text{SO}_3)_3$  to the same solution resulted in the appear-

ance of a new set of redox waves at ca. 500 mV vs. Ag/AgNO<sub>3</sub> (0.010 M) (Fig. 1(b)).

The current associated with the new redox couple increased linearly with the concentration of Y<sup>3+</sup> ion until a full equivalent had been added. At this point the original set of waves disappeared and the new redox couple reached full development (Fig. 1(c)). This indicates that the second wave results from the reversible oxidation of the ferrocenyl subunit in the (1): Y<sup>3+</sup> complex, with a 1:1 (ligand:cation) stoichiometry. The anodic shift of potential ( $\Delta E_{1/2}$ ) between the complex and the free ligand indicates the magnitude of the effect of the complexed cation on the redox potential of the cryptand. It is also a measure of electrostatic repulsion between the complexed cation and the electrogenerated positive charge in the oxidised form of the ferrocenyl subunit.

Qualitatively similar voltammetric behaviour was observed for the interaction of (1) with Na<sup>+</sup>, Ca<sup>+</sup> and Mg<sup>2+</sup> but no change was found in the presence of K<sup>+</sup>. As the charge on the cation increases, so does the observed shift in redox potential ( $\Delta E_{1/2}$ ) of the complex compared to the free ligand (Table 2(a)) and a plot of  $\Delta E_{1/2}$  vs.  $c/r$  is linear (Fig. 2). The correlation with  $c/r$  suggests that the shift in redox potential is due to transmission of charge from ferrocene to the bound

cation by polarisation of the conjugated carbonyl ligand thus confirming the conclusions of NMR and X-ray crystallographic studies [5,8,10,18].

The cyclic voltammogram of (2) exhibits a half-wave potential at -95 mV vs. Ag/AgNO<sub>3</sub> for the reversible oxidation of the ferrocenyl group. Gokel and coworkers have already reported that the CV behaviour of (2) is greatly affected by alkali metal cations in a 1:1 stoichiometry in acetonitrile, in which the  $\Delta E_{1/2}$  values were linearly proportional to the charge density ( $c/r^2$ ) of the bound cations [17] (Table 2b). Our observations agree with their report, but in addition we observe substantial anodic shifts on addition of Mg<sup>2+</sup> and Y<sup>3+</sup>. A plot of  $\Delta E_{1/2}$  values vs.  $c/r^2$  for the cations K<sup>+</sup>, Na<sup>+</sup>, Ca<sup>+</sup>, Mg<sup>2+</sup> and Y<sup>3+</sup> is also linear (Fig. 3) and it should be noted that in this case, the  $\Delta E_{1/2}$  value for the small Mg<sup>2+</sup> cation is actually greater than that for the more highly charged yttrium cation.

From the crystal structure and the NMR data of the {2(1); Y<sup>3+</sup>} complex [18] it is clear that the Y<sup>3+</sup> cation is coordinated by the amide carbonyl bonds of (1), and the same probably applies to all the other cations. Thus the transfer of electron density between the bound cation and the redox-active ferrocenyl group must be through the carbonyl bonds conjugated with the Cp rings (Fig. 4), and will therefore depend on the polarizing power of

Table 2  
Values of  $\Delta E_{1/2}$  (mV) and  $K_1/K_2$  for the complexation of (1)–(8) with cations in MeCN at 25°C

Cation	K <sup>+</sup>	Na <sup>+</sup>	Ca <sup>2+</sup>	Mg <sup>2+</sup>	Y <sup>3+</sup>
Radius, $r$ (Å)	1.330	0.970	0.990	0.660	0.893
$c/r$	0.752	1.031	2.020	3.030	3.359
$c/r^2$	0.565	1.063	2.040	4.519	3.761
(a) Compound (1)					
$\Delta E_{1/2}$ (mV)	–	19	98	174	225
$K_1/K_2$	–	2.18	49	970	$6.4 \times 10^3$
(b) Compound (2)					
$\Delta E_{1/2}$ (mV)	120	195	291	673	569
$K_1/K_2$	107	$1.98 \times 10^3$	$8.3 \times 10^4$	$2.4 \times 10^{11}$	$4.1 \times 10^9$
(c) Compound (3)					
$\Delta E_{1/2}$ (mV)	10	29	108	217	255
$K_1/K_2$	1.5	3.1	67	$4.65 \times 10^3$	$2.04 \times 10^4$
(d) Compound (4)					
$\Delta E_{1/2}$ (mV)	37	72	167	535	368
$K_1/K_2$	42	16	665	$1.3 \times 10^9$	$1.7 \times 10^6$
(e) Compound (5)					
$\Delta E_{1/2}$ (mV)	10	18	155	295	346
$K_1/K_2$	1.5	2.0	419	$9.7 \times 10^4$	$7.1 \times 10^5$
(f) Compound (6)					
$\Delta E_{1/2}$ (mV)	38	77	164	425	351
$K_1/K_2$	4.4	20	592	$1.5 \times 10^7$	$8.6 \times 10^5$
(g) Compound (7)					
$\Delta E_{1/2}$ (mV)	6	24	124	211	225
$K_1/K_2$	1.3	2.5	125	$4.3 \times 10^3$	$6.87 \times 10^3$
(h) Compound (8)					
$\Delta E_{1/2}$	–	36	86	292	202
$K_1/K_2$	–	4.1	28.4	$8.6 \times 10^4$	$2.6 \times 10^3$

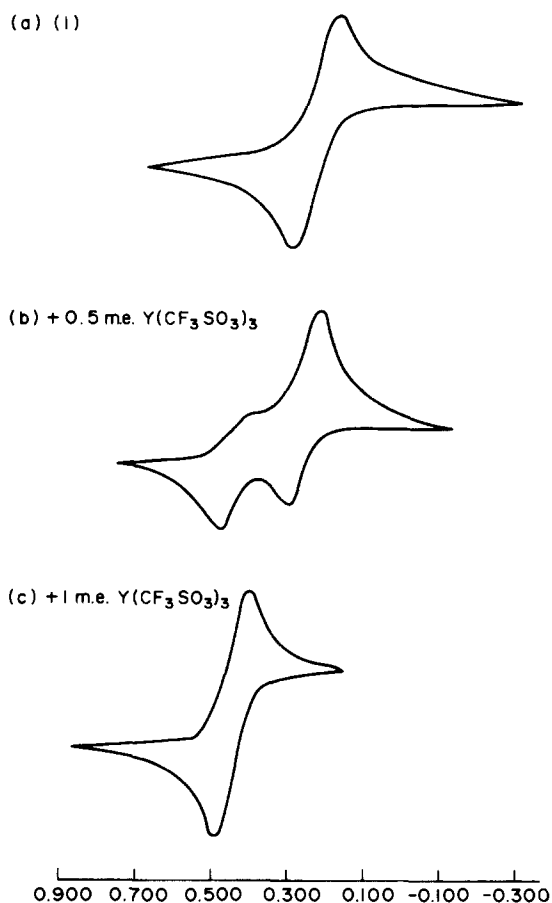
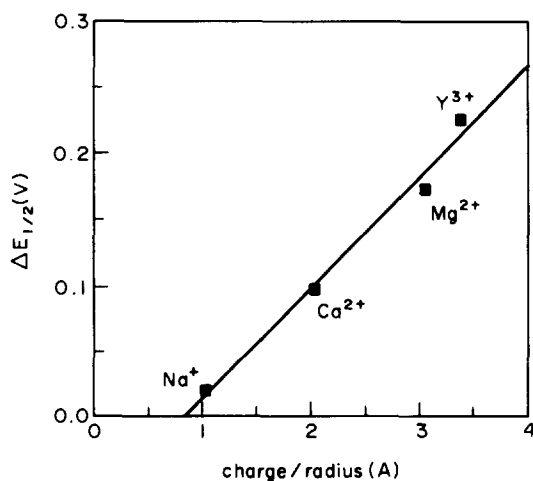
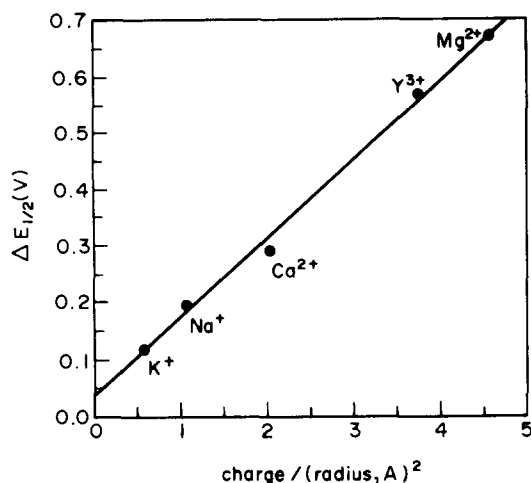


Fig. 1.

the cation. This is confirmed by the dependence of the  $\Delta E_{1/2}$  values on the ratio  $c/r$ , which is proportional to the polarisation of the carbonyl group by the cation.

In contrast, (2) contains no carbonyl bonds but has the unique structural feature of a well-formed cavity which facilitates the formation of encapsulated metal cation complexes (Fig. 5).

Fig. 2. Plot of  $\Delta E_{1/2}$  vs.  $c/r$  for complexes of (1) with various cations.Fig. 3. Plot of  $\Delta E_{1/2}$  vs.  $c/r^2$  for complexes of (2) with various cations.

The transfer of electron density is predicted to be through space between the bound cation and the ferrocene unit and will therefore depend on the charge density on the cation. This is substantiated by the CV data, since the  $\Delta E_{1/2}$  values for complexation of (2) with various cations are directly proportional to  $c/r^2$  which in turn is proportional to charge density. It should also be noticed that the range of  $\Delta E_{1/2}$  values for complexes of (1) is 20–230 mV ( $Na^+$  to  $Y^{3+}$ ), but the range of  $\Delta E_{1/2}$  values for complexes of (2) is much greater at 120–670 mV ( $Na^+$ – $Mg^{2+}$ ). This shows that the effect of the cation on the redox behaviour of the ferrocene unit is stronger with (2) than with (1). It is possible that with the reduced cryptand (2) there is some direct interaction between the cations and the iron atom which results in higher anodic shifts on complexation. Mössbauer studies are in progress in an attempt to verify this hypothesis but it should be noted that al-

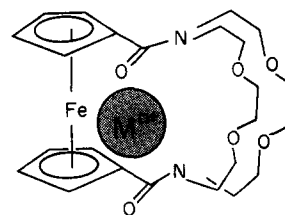


Fig. 4.

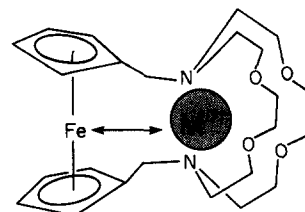


Fig. 5.

though Gokel et al. [17] found evidence for interaction between  $\text{Ag}^+$  and the ferrocenyl ion ( $\text{Ag}^+-\text{Fe} = 3.374 \text{ \AA}$ , X-ray crystallographic data suggested there was no interaction between the iron atom of (2) and  $\text{Na}^+$  ( $\text{Fe}-\text{Na}^+ = 4.39 \text{ \AA}$ ). The alternative explanation is that in cryptands derived from (2) the cations are in closer proximity to the iron atom than in cryptates derived from (1). The limited crystallographic data seems to support this contention since in the 2:1 (ligand:cation) complex of (1) with  $\text{Y}^{3+}$ , the  $\text{Fe}-\text{Y}^{3+}$  distances are 4.51 and 4.96  $\text{\AA}$  [18] which, on average, is significantly longer than the iron-cation distance found in the  $\text{Na}^+$  complex of (2). In a similar ferrocene-amide complex [11], the average  $\text{Fe}-\text{Ca}^{2+}$  distance was 5.0  $\text{\AA}$ .

Analogous CV studies with the monomers (3 and 4) and the dimers (5–8) are reported below with the monomers and dimers forming complexes with cations in a stoichiometry of 1:1 and 1:2 (ligand:cation), respectively.

### 3.2. Cyclic voltammetry of (5) and (6) in the presence of metal cations

Both (5) and (6) show a single set of CV waves centred at 296 mV and 21 mV respectively vs.  $\text{Ag}/\text{AgNO}_3$  which corresponds to the simultaneous oxidation of both ferrocenyl moieties within the molecules. There is no evidence of a second wave in either case, thus suggesting that oxidation of one ferrocene unit has no observable effect on the oxidation of the second. The addition of  $\text{Y}^{3+}$  to either of the ligands formed a new redox couple, and the new half-wave potential of the complex appeared as expected, at more positive values. Addition of one equivalent of  $\text{Y}^{3+}$  to (5) shifted the potential to an absolute value of 642 mV and a similar experiment with (6) gave a shift to 372 mV. The peak currents of the redox couple of {5;  $\text{Y}^{3+}$ } and {6;  $\text{Y}^{3+}$ } then increased with increasing  $[\text{Y}^{3+}]$  until they reached

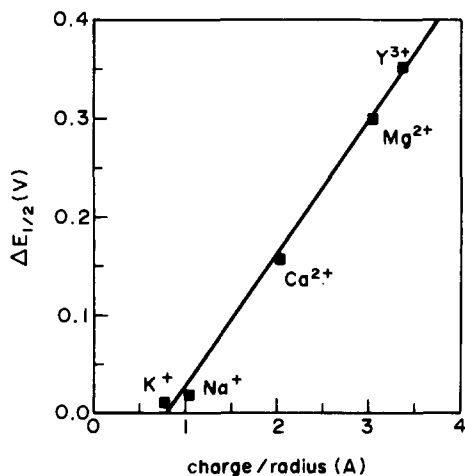


Fig. 6. Plot of  $\Delta E_{1/2}$  vs.  $c/r$  for complexes of (5) with various cations.

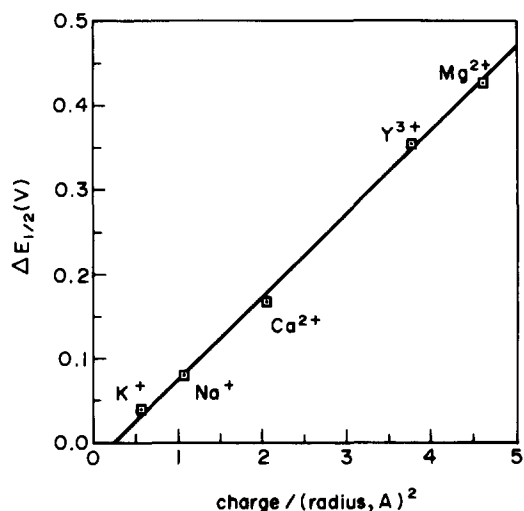


Fig. 7. Plot of  $\Delta E_{1/2}$  vs.  $c/r^2$  for complexes of (6) with various cations.

full development when  $[\text{Y}^{3+}]$  was exactly twice the concentration of the ligand, which indicated that both (5) and (6) complexed with  $\text{Y}^{3+}$  in a stoichiometry of 1:2 (ligand:cation). Plots of  $\Delta E_{1/2}$  vs.  $c/r$  for (5) (Fig. 6) and  $c/r^2$  for (6) (Fig. 7) for the cations  $\text{K}^+$ ,  $\text{Na}^+$ ,  $\text{Ca}^{2+}$ ,  $\text{Mg}^{2+}$  and  $\text{Y}^{3+}$  are linear. These observations show that both ligands are effective redox active cation sensors and once again, it should be noted that the shift for  $\text{Mg}^{2+}$  is greater than that for  $\text{Y}^{3+}$  with the reduced cryptand whereas the reverse is true for the nonreduced dimer (5) (Table 2e,f).

### 3.3. Cyclic voltammetry of (3), (4), (7) and (8) in the presence of metal cations

Cryptands (3), (4), (7) and (8) exhibit similar CV behaviour to that of their symmetrical analogues since

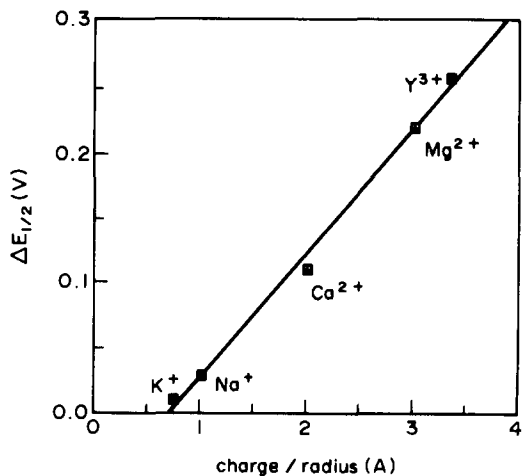


Fig. 8. Plot of  $\Delta E_{1/2}$  vs.  $c/r$  for complexes of (3) with various cations.

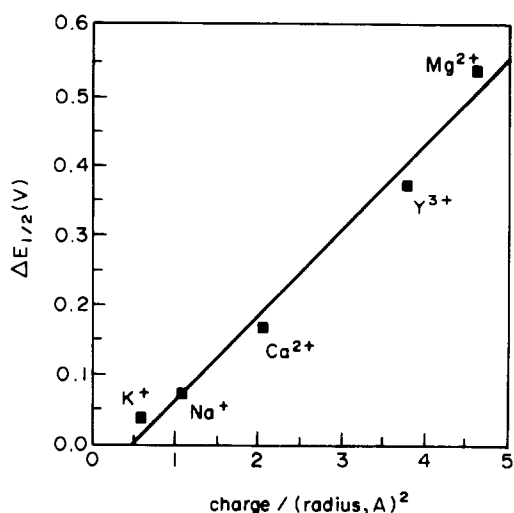


Fig. 9. Plot of  $\Delta E_{1/2}$  vs.  $c/r^2$  for complexes of (4) with various cations.

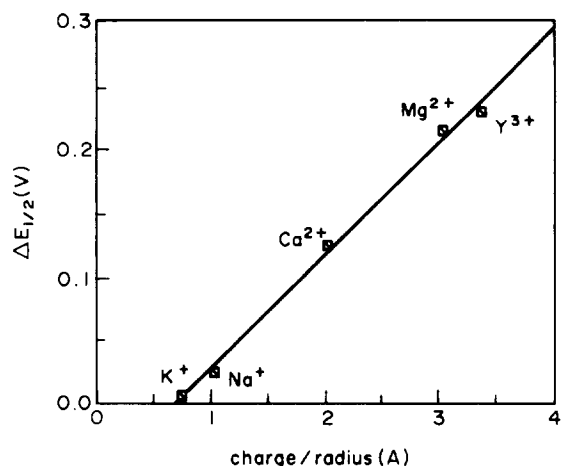


Fig. 10. Plot of  $\Delta E_{1/2}$  vs.  $c/r$  for complexes of (7) with various cations.

they each show a single set of waves at 249, -107, 295 and -83 mV respectively, for the reversible oxidation of the ferrocenyl group relative to Ag/AgNO<sub>3</sub>. The monomers and dimers again complex with cations in a stoichiometry of 1:1 and 1:2 (ligand:cation) respectively. Plots of  $\Delta E_{1/2}$  vs.  $c/r$  {for (3) (Fig. 8); and for (7) (Fig. 10)} and  $c/r^2$  {for (4) (Fig. 9) and for (8) (Fig. 11)} for the cations K<sup>+</sup>, Na<sup>+</sup>, Ca<sup>2+</sup>, Mg<sup>2+</sup> and Y<sup>3+</sup> are again linear. These observations show that the ligands are effective cation redox active sensors and once again, it should be noted that the shifts for Mg<sup>2+</sup>

are greater than those for Y<sup>3+</sup> when complexed with the reduced cryptands (Table 2c,d,g,h).

The data show that sizes of the amide (nonreduced) ligands (whether monomeric or dimeric, unsymmetrical or symmetrical) have little effect on the  $\Delta E_{1/2}$  values, but the latter are dependent on the ratio  $c/r$  which is proportional to polarisation of the carbonyl group by the cation. This confirms that the carbonyl bonds of these ligands transmit the withdrawal of electron density from the redox active ferrocenyl unit to the bound cations. The reduced forms of the ligands however, have  $\Delta E_{1/2}$

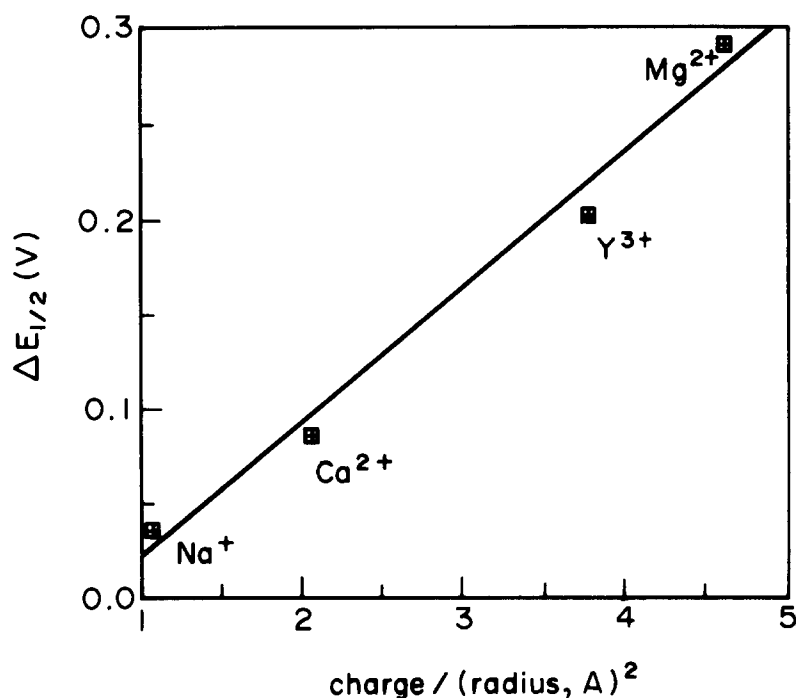


Fig. 11. Plot of  $\Delta E_{1/2}$  vs.  $c/r^2$  for complexes of (8) with various cations.

